Partial Differential Equations in Applied Mathematics 8 (2023) 100568

Contents lists available at ScienceDirect

Partial Differential Equations in Applied Mathematics

journal homepage: www.elsevier.com/locate/padiff

Fibonacci wavelet method for the numerical solution of a fractional relaxation–oscillation model

Shah Jahan [a], Shahid Ahmed [a], Pooja Yadav [a], Kottakkaran Sooppy Nisar [b,*]

[a] Department of Mathematics, Central University of Haryana, Mahendergarh 123029, India
[b] Department of Mathematics, College of Science and Humanities in Alkharj, Prince Sattam Bin Abdulaziz University, Kingdom of Saudi Arabia

ARTICLE INFO

MSC:
34A12
65M70
92D25
42C40

Keywords:
Fibonacci wavelet
Fractional calculus
Operational matrices
Viscoelasticity
Relaxation–oscillation equations

ABSTRACT

In this paper, we have discussed the Fibonacci wavelet (FW) framework for numerical simulations of the fractional relaxation–oscillation model (FROM). Firstly, the fractional order operational matrices of integration associated with the FW are constructed via the block pulse functions. The operational matrices merged with the collocation method are used to convert the given problem into a system of algebraic equations that is solved by the Newton method. We conduct error analysis, perform numerical simulations, and present the corresponding results to establish the credibility and practical applicability of the proposed technique. Numerical examples are provided to show the efficiency of our approach. To show the accuracy of the FW-based numerical technique, the approximate solutions of FROM are compared with the exact solution and other existing methods. This research opens up new possibilities for using FW as a powerful tool for addressing complex mathematical problems in real-world systems.

1. Introduction

Fractional calculus (FC) is dealing with the calculus of derivatives and integrals of arbitrary order either real or complex[1,2] There has been a powerful development in fractional differential equations (FDEs) in last few decades due to their applicability in different areas of science and engineering. Modelling biological models with fractional-order differential equations has more convenience than classical integer-order mathematical modelling. Many substantial efforts have been made to model and control biological systems using FDEs.[1,3–7] FDEs have an advantage in modelling of real-life phenomena because they reduce the errors arising from the ignored parameters. There are numerous examples of the mathematical model of biology, physical, natural and other fields of science that are represented by the FDEs.[3,7–12] Fractional calculus deals with derivatives and integrals of non-integer order, allowing it to capture memory and non-locality in a more comprehensive way than traditional integer-order calculus, which only considers the present state of a system. The fractional model combines the Caputo derivative, which accounts for present memory, and the Riemann–Liouville integral, which accounts for past memory, to describe systems with complex memory and non-local characteristics. This modelling approach is particularly useful in situations where traditional integer-order calculus models fall short, such as in the description of materials with memory effects, viscoelastic behaviour, or systems exhibiting long-range dependence and persistence. Fractional models provide a more accurate representation of how such systems evolve over time by incorporating both present and past memory. Fractional-order viscoelasticity models have proven to be very useful for simulating polymers. Polymers often behave in a time-dependent, inelastic manner that includes damping, relaxation, and creep. To replace costly experiments with numerical simulations, we require an accurate material model. One difficulty in particular that has been thoroughly researched is how highly detailed the viscoelastic material model must be or what the absolute minimum of parameters required for an accurate depiction of the material behaviour. There is little frequency dependence in the damping properties of many technological materials, especially polymers, across a broad frequency range. It is difficult to explain this weak frequency dependence in the framework of conventional viscoelastic models based on integer-order rate laws, at least without utilising an excessive number of material characteristics. Fractional order operators (integrals and derivatives) can be incorporated in the constitutive relations as an alternative to employing integer order operators. The number of parameters required to correctly define the dynamic characteristics can be considerably reduced as a result.[13–15]

Natural and artificial soft materials are frequently viscoelastic, having memory and fractionally frequency-dependent characteristics. Their two most prevalent mechanical characteristics are stress relaxation and damped oscillation.[15–17] A relaxation oscillator is a type of oscillator

* Corresponding author.
E-mail addresses: Shahjahan@cuh.ac.in (S. Jahan), n.sooppy@psau.edu.sa (K.S. Nisar).

https://doi.org/10.1016/j.padiff.2023.100568
Received 22 July 2023; Received in revised form 29 September 2023; Accepted 30 September 2023
Available online 5 October 2023

that is based on the way that perturbed physical systems recover to equilibrium. Physics is strongly connected to the two fundamental phenomena of relaxation and oscillation in their processes.[8,18,19] The principal equation governing relaxation and oscillation processes is the relaxation–oscillation equation.

$$\frac{d\mu}{dx} + P\mu = f(x), \quad x \geq 0. \tag{1.1}$$

Where P stands for Elc, the elastic modulus is represented by E, the viscous coefficient is denoted by c, and E multiplied by the strain rate is represented by the symbol f(x). The viscoelastic behaviour Maxwell model is represented by Eq. (1.1) and the analytical solutions for $f(x) = 0$ are

$$\mu(x) = Cexp(-Px). \tag{1.2}$$

The natural exponential stress relaxation under continuous strain is described by Eq. (1.2), where C is a constant specified by the starting state. The usual oscillation formula

$$\frac{d^2\mu}{dx^2} + Q\mu = f(x), \quad x \geq 0. \tag{1.3}$$

Where $Q\ is\ \ k/m = \omega^2$, ω is the angular frequency, k and m are stiffness coefficient and mass, respectively. When we take $f(x) = 0$ the exact solution is

$$\mu(x) = C\cos\sqrt{Q}x + D\sin\sqrt{B}x. \tag{1.4}$$

Here the initial condition determines the constants C and D. The system is conservative and the model depicts undamped oscillation. The relaxation and oscillation models use fractional positive fractional and fractal derivatives to depict gradual relaxation and damped oscillation.[16,18,19] In this article we used fractional derivatives for the corresponding models (1.1) and (1.2) which give FROM as

$$\frac{d^\alpha\mu}{dx^\alpha} + Q\mu(x) = f(x), \quad x \geq 0. \tag{1.5}$$

Q denotes a positive constant. This FROM depicts the relaxation with power law attenuation at $0 < \alpha < 1$. At $1 < \alpha < 2$, the FROM illustrates a damped oscillation with viscoelastic intrinsic oscillator damping.[19] In fact, the classic relaxation and oscillation models use fractional derivatives to demonstrate gradual relaxation and damped oscillation. This fractional model is frequently employed in a number of related disciplines, including physical oscillation systems and nonlinear dynamic systems. It has been demonstrated to be a mathematical representation of a number of physical processes, including diffusion,[20] the spruce-budworm system,[21] the predator–prey system,[22] the damping law and others.[18,22] Finding a solution to FROM is becoming a hot topic for researchers. As it involves specific functions like multivariable Mittag-Leffler functions, which are particularly challenging to compute. As a result, the significance of successful numerical modelling using the FROM has increased in related research fields.[18–22] The creation of reliable techniques for solving fractional order relaxation–oscillation equations numerically has received a lot of interest recently. Some of the numerical techniques include Muntz-Legendre wavelets approach,[23] a computational algorithm for simulating fractional order relaxation oscillation equation,[24] a new accurate method for solving FROM with Hifler derivatives,[25] differential transform method,[26] Homotopy asymptotic method and others. In the literature there are not much publication dealing with the numerical treatment of FROM using wavelets. Wavelets have found applications in various areas, including signal and image processing, data compression, scientific computing, and solving differential and integral equations.[20,27,28] They offer advantages over traditional methods by allowing for adaptive and multiscale analysis, which can capture both global and local features of the problem. Wavelets based numerical approaches have been carefully examined and applied in a wide range of scientific and engineering fields, offering a powerful and flexible framework for numerical analysis and computation. In recent years, wavelet techniques have been widely employed by researchers to solve fractional-order differential equations. The popularity of wavelet-based numerical algorithms can be attributed to their straightforwardness, computational simplicity, and speedy convergence. Various types of wavelets have been explored in the literature, including Chebyshev, Gegenbaur,[29] Bernoulli, Haar,[28] and FW[30–32] are consistently used to solve various biological and physical problems.[27,33–35] The main objective of this study is to present a numerical technique for the solution of FROM based on the FW operational matrix approach. In this paper, we proposed Fibonacci wavelet method (FWM) to solve FROM. Fibonacci polynomials can be directly obtained as a special case of the generalised Fibonacci polynomials which originally appeared in the numerical solution of differential equations in Ref. 3. The Fibonacci polynomials has gained significant attention due to their superior characteristics compared to the Legendre polynomials. The FW consist of fewer terms as compared to other polynomial wavelets which accelerates computation and reduces the chances of errors occurring. This motivates us to use Caputo fractional derivatives and FW based methods to understand and analyse FROM. The proposed approach offers a comprehensive framework for accurately modelling and analysing the behaviour of fractional order dynamics in the system. Further we discussed convergence and error analysis and presented numerical examples to show the efficiency of the proposed method. Our results reveal that the present approach agrees perfectly with the conventional techniques.[24,26]

The rest of the paper is organised as: In Section 2 the mathematical preliminaries of fractional calculus is discussed. Section 3 presents an overview of the FW and function approximation. In Section 4 the block pulse functions and operational matrix of FW are discussed. In Section 5, the description of the proposed technique is obtained. Section 6, the error estimation and numerical problems are discussed to demonstrate the effectiveness and accuracy of the proposed approach. Lastly, a conclusion is given in Section 7.

2. Fractional calculus

Various techniques for defining fractional order derivatives, including Caputo, Riemann–Liouville(RL), Baleno fractional, and Grünwald–Letnikov. Since most physical processes begin with starting conditions specified in form of field coordinates and its integer order, Caputo's method is remarkable. To avoid confusion, the fractional derivative will be used throughout the rest of this article in the sense of Caputo. For further studies, we refer Refs. 36, 37.

Definition 2.1. The fractional integral of RL type of order $\alpha > 0$ of a function $g(x)$ is

$$I^\alpha g(x) = \frac{1}{\Gamma(\alpha)} \int_0^x (x-\tau)^{\alpha-1} g(\tau)\, d\tau, \quad x > 0.$$

Where $\Gamma(.)$ is the gamma function. Few, properties of I^α are listed below:

- $I^\alpha I^\beta g(x) = I^{\alpha+\beta} g(x), \qquad \alpha, \beta > 0.$
- $I^\alpha I^\beta g(x) = I^\beta I^\alpha g(x), \qquad \alpha, \beta > 0.$
- $I^\alpha x^\beta = \dfrac{\Gamma(1+\beta)}{\Gamma(1+\alpha+\beta)} x^{\alpha+\beta}, \qquad \beta > -1.$

Definition 2.2. The fractional derivative D^α of order α in the sense of Caputo of $g(x)$ is defined as

$$D^\alpha g(x) = \frac{1}{\Gamma(n-\alpha)} \int_0^x \frac{g^n(\tau)}{(x-\tau)^{\alpha-n+1}}\, d\tau, \quad n-1 < \alpha \leq n, n \in \mathbb{N}.$$

Below are some fundamental features of D^α:

- $D^\alpha\big(\gamma g(x) + \delta g(x)\big) = \gamma D^\alpha g(x) + \delta D^\alpha g(x)$, where γ, δ are constants.
- $D^\alpha x^\beta = \dfrac{\Gamma(1+\beta)}{\Gamma(1+\beta-\alpha)} x^{\beta-\alpha}, \quad 0 < \alpha < \beta+1, \quad \beta > -1.$
- $I^\alpha D^\alpha g(x) = g(x) - \sum_{k=0}^{n-1} f^k(0^+) \dfrac{x^k}{k!}, \quad n-1 < \alpha \leq n, \quad n \in \mathbb{N}.$
- $D^\alpha C = 0, \quad C$ is a constant.

3. Fibonacci wavelet and function approximation

For any $x \in \mathbb{R}^+$, the recurrence relation defines the Fibonacci polynomials as follows:

$$\tilde{P}_{n+2}(x) = x\tilde{P}_{n+1}(x) + \tilde{P}_n(x), \quad (n \in \mathbb{N}),$$

with initial conditions $\tilde{P}_0(x) = 0, \tilde{P}_1(x) = 1$.[30]

The general formula used to define Fibonacci polynomial as follows:

$$\tilde{P}_{m+1}(x) = \begin{cases} 1 & n = 0, \\ x & n = 1, \\ x\tilde{P}_n(x) + \tilde{P}_{n-1}(x) & n \geq 2. \end{cases}$$

The FW is defined as:

$$\Psi_{n,n}(x) = \begin{cases} \frac{2^{\frac{k-1}{2}}}{\sqrt{w_n}} \widehat{P}_n\left(2^{k-1}x - n + 1\right) & \frac{n-1}{2^{k-1}} \leq x < \frac{n}{2^{k-1}}, \\ 0 & \text{otherwise.} \end{cases} \tag{3.1}$$

where k and n represent the level of resolution and translation parameters respectively, with $k = 1, 2, 3, \ldots$, $n = 1, 2, 3, \ldots, 2^{k-1}$, and $\tilde{P}_n$ is the m- degree polynomials.[30]

Additionally, the Fibonacci polynomials power-form representation appears as follow:

$$\tilde{P}_n(x) = \sum_{i=0}^{\lfloor n/2 \rfloor} \binom{n-i}{i} x^{n-2i}, \quad (n \geq 0),$$

where $\lfloor \cdot \rfloor$ stands the well recognised floor function. The Fibonacci polynomial has the following properties:

$$\int_0^x \tilde{P}_n(s)ds = \frac{1}{n+1}\left[\tilde{P}_{m+1}(x) + \tilde{P}_{n-1}(x) - \tilde{P}_{n+1}(0) + \tilde{P}_{n-1}(0)\right].$$

$$\int_0^1 \tilde{P}_n(x)\tilde{P}_m(x)dx = \sum_{i=0}^{\lfloor n/2 \rfloor}\sum_{j=0}^{\lfloor m/2 \rfloor} \binom{n-i}{i}\binom{m-j}{j} \frac{1}{n+m-2i-2j+1}. \tag{3.2}$$

In particular, if $k = 2, \quad M = 4$, the eight basis functions are given by

$$\left.\begin{aligned} \psi_{1,0}(x) &= \sqrt{2} \\ \psi_{1,1}(x) &= 2\sqrt{6}x \\ \psi_{1,2}(x) &= \sqrt{\tfrac{15}{14}}\left(1 + 4x^2\right) \\ \psi_{1,3}(x) &= \sqrt{\tfrac{960}{38}}\left(2x^3 + x\right) \end{aligned}\right\} \quad 0 \leq x < \frac{1}{2},$$

$$\left.\begin{aligned} \psi_{2,0}(x) &= \sqrt{2} \\ \psi_{2,1}(x) &= \sqrt{6}(2x - 1) \\ \psi_{2,2}(x) &= \sqrt{\tfrac{30}{7}}\left(2x^2 - 2x + 1\right) \\ \psi_{2,3}(x) &= \sqrt{\tfrac{480}{304}}\left(8x^3 - 12x^2 + 10x - 3\right) \end{aligned}\right\} \quad \frac{1}{2} \leq x < 1.$$

Any function $f \in L^2[0, 1)$ can be expressed using the FW as

$$f(x) \approx \sum_{m=1}^{2^{k-1}}\sum_{n=0}^{M-1} g_{m,n}\psi_{m,n}(x). \tag{3.3}$$

Where

$$g_{m,n} = \left\langle f, \psi_{m,n}\right\rangle = \int_0^1 f(x)\psi_{m,n}(x)dx,$$

are the coefficients of FW. The following is how (3.3) expressed as a matrix

$$f(x) = G^T\Psi(x), \tag{3.4}$$

where G is the row vector defined below

$$G = \left[g_{1,0}, g_{1,1}, \ldots, g_{1,M-1}, g_{2,0}, g_{2,1}, \ldots, g_{2,M-1}, \ldots, g_{2^{k-1},0}, g_{2^{k-1},1}, \ldots, g_{2^{k-1},M-1}\right]^T. \tag{3.5}$$

The matrix $\Psi(x)$ in (3.4) is of order $1 \times 2^{k-1}M$ FW matrix and is given by

$$\Psi(x) = \left[\psi_{1,0}, \psi_{1,1}, \ldots, \psi_{1,M-1}, \psi_{2,0}, \psi_{2,1}, \ldots, \psi_{2,M-1}, \ldots, \psi_{2^{k-1},0}, \psi_{2^{k-1},1}, \ldots, \psi_{2^{k-1},M-1}\right]^T. \tag{3.6}$$

Finally, we take into account the collocation point:

$$x_\ell = \frac{2\ell - 1}{2^k M}, \quad \ell = 1, 2, \ldots, 2^{k-1}M. \tag{3.7}$$

The choice of collocation points(nodes) can have a significant impact on the accuracy and efficiency of numerical methods. It is essential to carefully consider the problem's characteristics and requirements when selecting collocation nodes to ensure that they lead to accurate, stable, and efficient solutions.

4. Operational matrices of Fibonacci wavelet

Utilising block-pulse functions is the goal of this section to produce integration operational matrices of fractional order for FW is discussed.

4.1. Block pulse function

On the interval $[0, 1)$, the block-pulse functions are defined as

$$b_\ell(x) = \begin{cases} 1, & \ell q \leq x < (\ell + 1)q, \\ 0, & \text{otherwise.} \end{cases} \tag{4.1}$$

where $q = \frac{1}{N}$ and N is positive integer $\ell = 0, 1, 2, \ldots, N - 1$.

The function $f(x) \in L^2[0, 1)$ estimated via of block plus function.

$$f(x) \simeq f_N(x) = \sum_{\ell=1}^{N-1} a_\ell b_\ell(x) = A^T C_N, \tag{4.2}$$

where $C_N = [C_0, C_1, C_2, \ldots, C_N]^T$ and $A = [a_0, a_1, a_2, \ldots, a_N - 1]$. Integrating the vector $C_N(x)$, we obtain

$$\int_0^x C_N(x)dx \simeq \Delta C_N(x). \tag{4.3}$$

The integration operational matrix for block pulse functions is defined as follow

$$\Delta = \frac{q}{2}\begin{pmatrix} 1 & 2 & 2 & \ldots & 2 \\ 0 & 1 & 2 & \ldots & 2 \\ \vdots & \vdots & \vdots & \cdots & \vdots \\ 0 & 0 & 0 & \cdots & 1 \end{pmatrix}. \tag{4.4}$$

Then, by using block pluse function to describes the operational matrix of fractional order F^α as

$$\left(I^\alpha C_N\right)(x) \simeq F^\alpha C_N(x), \tag{4.5}$$

where

$$F^\alpha = \frac{1}{N^\alpha\Gamma(\alpha + 2)}\begin{pmatrix} 1 & x_1 & x_2 & x_3 & \ldots & x_{N-1} \\ 0 & 1 & x_1 & x_2 & \ldots & x_{N-2} \\ 0 & 0 & 1 & x_1 & \ldots & x_{N-3} \\ \vdots & \vdots & \vdots & \vdots & \ldots & \vdots \\ 0 & 0 & \ldots & 0 & 1 & x_1 \\ 0 & 0 & 0 & \ldots & 0 & 1 \end{pmatrix}, \tag{4.6}$$

where, the x_ℓ 's in (4.6) have been defined as:

$$x_\ell = (\ell + 1)^{\alpha+1} - 2\ell^{\alpha+1} + (\ell - 1)^{\alpha+1}. \tag{4.7}$$

4.2. Operational matrix of FW

Using block pulse functions, we will next develop fractional order integration matrices related to FWs by integrating (3.6) we have

$$\int_0^x \Psi(x)dx \approx U\Psi(x). \tag{4.8}$$

Where U displays the integration operational matrix for $2^{k-1}M \times 2^{k-1}M$ order of FW. It is important to note that block-pulse functions (4.1) can also be used to represent the FWs (3.6) as

$$\psi(x) = \psi_{\mathrm{m,n}} C_N(x). \tag{4.9}$$

To obtain the integration operational matrix of α order for FW, we define

$$D^{\alpha}\psi(x) = U^{\alpha}_{\mathrm{m,n}}\psi(x), \tag{4.10}$$

where the matrix $U^{\alpha}_{\mathrm{m,n}}$ represent the FW's integration operational matrix in fractional order, taking into account the relationships (4.5), (4.9) and (4.10) we get

$$\left(D^{\alpha}\psi\right)(x) \approx \left(D^{\alpha}\psi_{\mathrm{m,n}}C_N\right)(x) = \psi_{\mathrm{m,n}}\left(D^{\alpha}C_N\right)(x) \approx \psi_{\mathrm{m,n}}F^{\alpha}C_N(\zeta). \tag{4.11}$$

Therefore, from (4.10) and (4.11), we get the following:

$$U^{\alpha}_{\mathrm{m,n}}\psi(x) = U^{\alpha}_{\mathrm{m,n}}\psi_{\mathrm{m,n}}C_N(x) = \psi_{\mathrm{m,n}}F^{\alpha}C_N(x), \tag{4.12}$$

which results in the necessary operational matrix for the FWs of general order integration:

$$U^{\alpha}_{\mathrm{m,n}} = \psi_{\mathrm{m,n}}F^{\alpha}\left[\psi_{\mathrm{m,n}}\right]^{-1}. \tag{4.13}$$

In particular, by taking $k = 2, M = 3, \alpha = 0.7$, we compute the associated fractional order operational matrix $U^{0.7}_{6\times6}$ corresponding with the FWs as:

$$U^{0.7}_{6\times6} = \begin{pmatrix} 0.2781 & 0.4872 & -0.3112 & 0.4426 & -0.2191 & 0.2527 \\ -0.5224 & 0.0947 & 0.7290 & 0.3752 & -0.2523 & 0.3088 \\ -0.0845 & 0.3015 & 0.1813 & 0.4247 & -0.2405 & 0.2857 \\ 0 & 0 & 0 & 0.2781 & 0.4872 & -0.3112 \\ 0 & 0 & 0 & -0.5224 & 0.0947 & 0.7290 \\ 0 & 0 & 0 & -0.0845 & 0.3015 & 0.1813 \end{pmatrix}. \tag{4.14}$$

Similarly, if we take $k = 2, M = 4$ and $\alpha = 0.6$, we compute $U^{0.6}_{8\times8}$ as:

$$U^{0.6}_{8\times8} = \begin{pmatrix} 0.9713 & 0.2499 & -1.2400 & 0.4341 & -0.1574 & -0.0143 & 1.1364 & -0.4158 \\ -0.8169 & 0.3068 & 1.1325 & -0.2138 & -0.4329 & 0.0334 & 1.5242 & -0.5715 \\ 0.5864 & 0.0052 & -0.7356 & 0.4852 & -0.2955 & 0.0091 & 1.3612 & -0.5050 \\ -0.6367 & -0.1470 & 0.8813 & 0.2610 & -0.6442 & 0.0588 & 2.1052 & -0.7929 \\ 0 & 0 & 0 & 0 & 0.9713 & 0.2499 & -1.2400 & 0.4341 \\ 0 & 0 & 0 & 0 & -0.8169 & 0.3068 & 1.1325 & -0.2138 \\ 0 & 0 & 0 & 0 & 0.5864 & 0.0052 & -0.7356 & 0.4852 \\ 0 & 0 & 0 & 0 & -0.6367 & -0.1470 & 0.8813 & 0.2610 \end{pmatrix}. \tag{4.15}$$

5. Description of method

Consider the standard harmonic fractional oscillator equation

$$\frac{d^{\alpha}\mu}{dx^{\alpha}} + Q\mu(x) = f(x), \quad 1 < \alpha \le 2,\ 0 \le x < 1, \tag{5.1}$$

with initial condition $\mu(0) = a$, and $\mu'(0) = b$, Eq. (5.1) presents a basic harmonic fractional oscillator. Expanding the higher order term of Eq. (5.1) we have

$$\frac{d^{\alpha}\mu}{dx^{\alpha}} = \sum_{m=0}^{M-1}\sum_{n=1}^{2^{k-1}} d_{m,n}U_{n,m}(\tau) = (D)^T U(x), \tag{5.2}$$

integrating (5.2) w.r.t x and using initial condition, we get

$$\mu(x) = \sum_{m=0}^{M-1}\sum_{n=1}^{2^{k-1}} d_{m,n}(I^{\alpha}_0 U_{n,m}(x)) + \mu(0) = (D)^T P^{\alpha}U(x) + x\mu'(0) + \mu(0), \tag{5.3}$$

substituting (5.2) and (5.3) into (5.1), we get the following system

$$(D)^T U(x) + Q((D)^T P^{\alpha}U(x) + x\mu'(0) + \mu(0)) = f(x), \tag{5.4}$$

solving the above algebraic equation, the unknown fibonacci coefficient vector $(D)^t$ is obtained, and the approximate solution of (5.1) is given by (5.3).

6. Error estimation and numerical results

In this section, we study the error estimation and convergence analysis of FWs technique. The convergence and error analysis of the Fibonacci polynomials as a basis functions was deeply studied in Refs. 3–6 Some numerical examples are presented to show the accuracy of the FWM.

Theorem 6.1 (*Ref. 31*). *Suppose $\Theta \in C^M[0,1)$ and $Y_M = span\{\psi_0(x), \psi_1(x), \ldots, \psi_{M-1}(x)\}$. If $\Theta_M(x) = A^T\hat{F}(x)$ is the best approximation of $\Theta(x)$ out of Y_M on the interval $[\frac{u-1}{2^{k-1}}, \frac{u}{2^{k-1}}]$ the error bound of the approximate solution $\Theta^*(x)$ by using FW on interval $[0,1)$ would be obtained in the following form:*

$$\|e(x)\|_2 = \left\|\Theta - \Theta^*\right\|_2 \le \frac{R}{M!\sqrt{2M+1}}.$$

Theorem 6.2 (*Ref. 31*). *If a continuous function $f(x)$ be a square integrable function defined on [0, 1) which is bounded by some constant $\tilde{M}$ i.e, $|f(x)| \le \tilde{M}$, then the function $f(x)$ can be expanded as the sum of FW and the series converges to $f(x)$ uniformly, i.e,*

$$f(x) = \sum_{\mathrm{m=1}}^{2^{k-1}}\sum_{\mathrm{n=0}}^{M-1} g_{\mathrm{m,n}}\psi_{\mathrm{m,n}}(x),$$

where

$$g_{\mathrm{m,n}} = \left\langle f(x), \psi_{\mathrm{m,n}}(x)\right\rangle.$$

The precision of the FW collocation methods is measured by the absolute error L_2 and maximum absolute errors L_∞ by using the formulas given as

$$L_2 = \|\mu(x) - \mu_m(x)\|,$$

$$L_\infty = max|\mu(x) - \mu_m(x)|,$$

where $\mu(x)$ and $\mu_m(x)$ are the exact and approximate solutions respectively.

6.1. Numerical results

Here, we go over the numerical outcomes of the suggested approach to solve the FROM (1.5). Some particular instances on Eq. (1.5) have been taken into account for representing the competence and relevancy of the suggested method. The following cases are taken into consideration since the literature already contains the analytical solutions to some of them. This enables us to compare our results to the analytical solution. All the computation work is performed using the MATLAB (R2022b) software.

Example 6.1. Take a look at the following relaxation–oscillation equation

$$D^{\alpha}\mu(x) + Q\mu(x) = f(x), \quad x > 0, \quad \mu(0) = \lambda, \tag{6.1}$$

subject to the conditions

$$\mu(0) = 1, \quad 0 < \alpha \le 1, \quad and \quad \mu(0) = 1,\ \mu'(0) = 0, \quad 1 < \alpha \le 2.$$

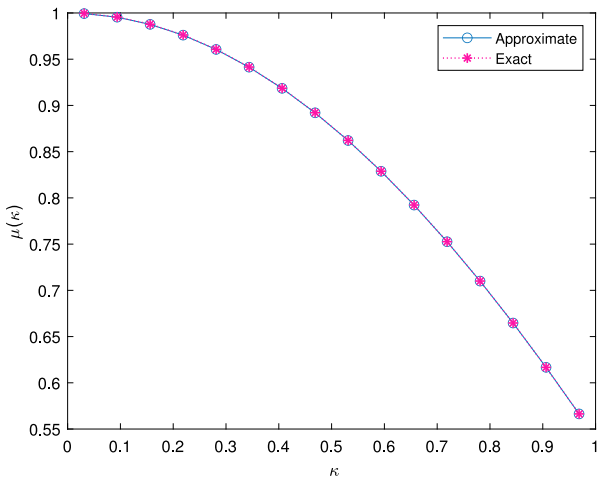

Fig. 1. Graphs of approximate and exact solutions at $\alpha = 2$.

Table 1
Absolute error at $\alpha = 2$ and at resolution level $k = 3, M = 4$ of Example 6.1.

x	$\alpha = 1$	$\alpha = 2$	Absolute error L_2
(0.2)	0.969697	0.999349	8.0752e−05
(0.3)	0.855720	0.987661	6.3710e−05
(0.4)	0.755139	0.960565	4.5413e−05
(0.5)	0.666380	0.918485	2.5982e−05
(0.6)	0.588055	0.862078	5.5483e−06
(0.7)	0.518935	0.792222	3.7848e−06
(0.8)	0.457940	0.710079	2.1453e−07
(0.9)	0.379622	0.616717	1.3328e−07

Table 2
Absolute error at resolution level $k = 3, M = 5$ of Example 6.2.

x	GTMM[38]	HAM[20]	Absolute error L_2 (FWM)
(0.2)	0.1358×10^{-4}	0.2096×10^{-4}	5.6680e−07
(0.3)	0.8375×10^{-4}	0.2292×10^{-4}	3.3044e−07
(0.4)	0.3037×10^{-3}	0.1484×10^{-3}	7.1240e−06
(0.5)	0.8230×10^{-3}	0.5838×10^{-6}	3.8040e−06
(0.6)	0.1854×10^{-2}	0.1289×10^{-4}	7.9070e−05

Exact solution is $\mu(x) = \cos(x)$.

In Fig. 1, we have compared the exact and approximate solution at $\alpha = 2$ of example 6.1. Fig. 2, depicts the behaviour of approximate solution at $\alpha = 1.25, 1.50, 1.75, 1.95$. The absolute error are presented in Table 1, at resolution level $k = 3, M = 4$ of Examples 6.1 shows the accuracy of the method.

Example 6.2. Consider the following

$$D^{3/2}\mu(x) + Q\mu(x) = 0, \quad 0 < x \le 1, \tag{6.2}$$

with following conditions

$$\mu(0) = 1, \quad \text{and} \quad \mu'(0) = 0.$$

Exact solution is $\mu(x) = E_\alpha(-x^\alpha)$ where

$$E_\alpha(x) = \sum_{k=0}^{\infty} \frac{x^k}{\Gamma(\alpha k + 1)}.$$

In Fig. 3, the comparison of exact and approximate solution are depicted of Example 6.2. The absolute error are calculated (see Table 2) and the results are compared with other methods[20,38] to show the efficiency of the methods. FWM give more precise solutions for these models.

Table 3
Absolute error at $\alpha = 1$ and at resolution level $k = 3, M = 4$ of Example 6.3.

x	GTMM[38]	Method in Ref. 24	Absolute error L_2 (FWM)
(0.2)	1.10×10^{-3}	1.10e−02	5.7041e−05
(0.3)	0.1002×10^{-2}	9.13e−03	4.2563e−05
(0.4)	0.2655×10^{-2}	9.84e−03	7.6321e−04
(0.5)	0.5638×10^{-2}	7.51e−03	3.4256e−04
(0.6)	0.1041×10^{-1}	4.60e−03	1.4770e−04

Table 4
Absolute error at $\alpha = 1$ and at resolution level $k = 4, M = 5$ of Example 6.4.

x	FWM k = 2, M = 4	FWM k = 3, M = 4	HAM[20]	DTM[26]
(0.2)	0.98617952	0.98684367	0.98712230	0.98712227
(0.3)	0.97336972	0.97408218	0.97442147	0.97442100
(0.4)	0.95707929	0.95799266	0.95844874	0.95844541
(0.5)	0.93787452	0.93863115	0.93956673	0.93955156
(0.6)	0.91594528	0.91659420	0.91807156	0.91801913
(0.7)	0.89150255	0.89167981	0.89423459	0.89408505
(0.8)	0.86433118	0.86424646	0.86833023	0.86795946

Example 6.3. Consider

$$D^{1/2}\mu(x) + Q\mu(x) = 0, \quad 0 < x \le 1, \tag{6.3}$$

with following conditions

$$\mu(0) = 1, \quad \text{and} \quad \mu'(0) = 0.$$

Exact solution is $\mu(x) = E_{1/2}(-x^{1/2})$ where

$$E_\alpha(\tau) = \sum_{k=0}^{\infty} \frac{\tau^k}{\Gamma(\alpha k + 1)}.$$

In Fig. 4, the comparison of exact and approximate solution are depicted of Example 6.3. The absolute error (see Table 3) are calculated and the results are compared with generalized taylor matrix method (GTMM)[24] and method in Ref. 38 to show the efficiency of the FW method.

In above three example we have considered the relaxation oscillation equations of fractional order with $Q = 1$. The results are plotted and also presented in Tables to shows the accuracy of the proposed method.

Example 6.4.
Consider the following

$$\frac{d^\alpha \mu}{dx^\alpha} + w^\alpha \mu(x) = f(x), \quad 1 \le \alpha \le 2, 0 \le x \le 1, \tag{6.4}$$

with conditions

$$\mu(0) = 1, \quad \mu'(0) = 0.$$

Example 6.5.

$$\frac{d^\alpha \mu}{dx^\alpha} + w^\alpha \mu(x) = \sin(wx), \quad 1 \le \alpha \le 2, 0 \le x \le 1, \tag{6.5}$$

with conditions

$$\mu(0) = 0, \quad \mu'(0) = 0.$$

In Examples 6.4 and 6.5, we considered fractional oscillator equations in which the exact solution is not known. Take, $w = 0.5, 0.3$ for Examples 6.4 and 6.5, respectively. In Fig. 5(a), the comparison of differential transform method (DTM)[26], Homotopy asymptotic method (HAM)[20] and FWM are presented. Also the behaviour of the FWM solutions at $\alpha = 1.8, 1.85, 1.9$ are shown in Fig. 5(b). In Table 4, absolute error is presented with different resolution levels and the results

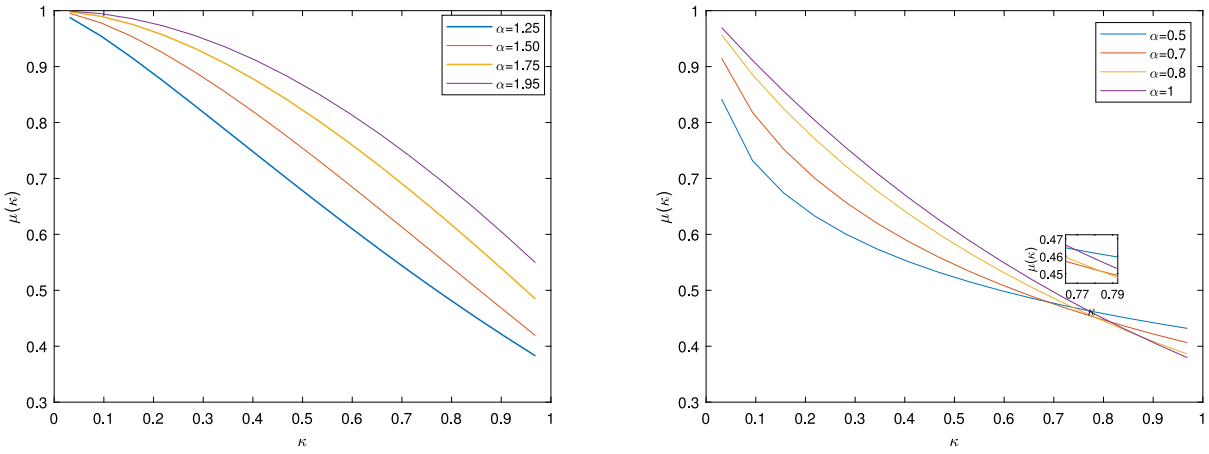

Fig. 2. (a) Behaviour of approximate solution when $1 < \alpha \leq 2$, (b) Behaviour of approximate solution when $0 < \alpha \leq 1$.

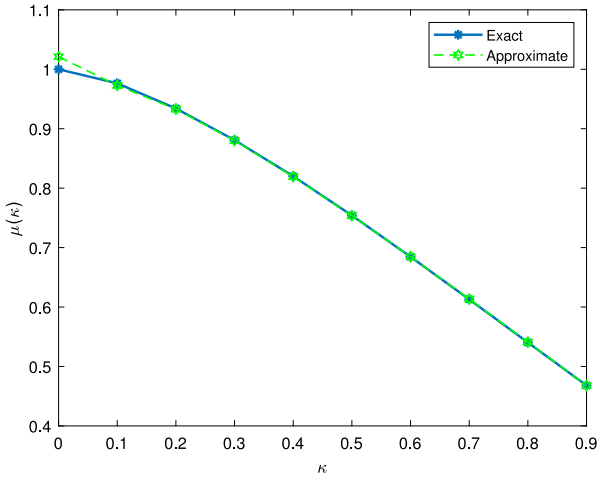

Fig. 3. Graph of exact and approximate solution.

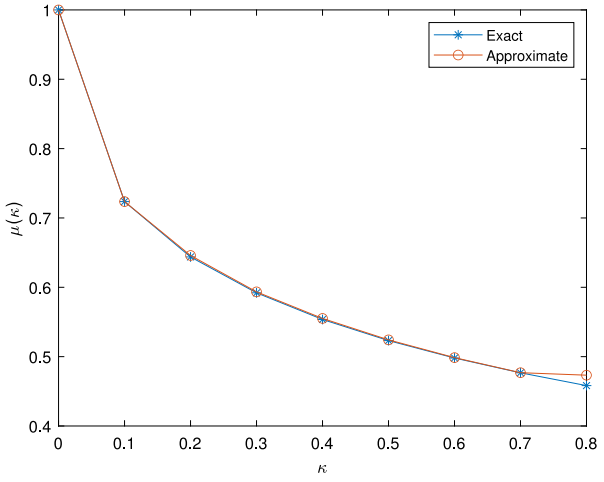

Fig. 4. Comparison of exact and approximate solutions.

are compared with other existing methods.[22,38] For Example 6.5, the Fig. 6(a) shows the comparison of HAM and FW approximate solutions. Also the behaviour of the FW approximate solution is presented at different values of α in Fig. 6(b).

Example 6.6. Consider the following nonlinear fractional oscillator equation

$$\frac{d^{\alpha}\mu(x)}{dx^{\alpha}} + 2\mu(x) + \mu^{2}(x) = 0, \quad 1 < \alpha \leq 2, \quad 0 \leq x < 1, \tag{6.6}$$

with conditions $\mu(0) = 0.1$, $\mu'(0) = 0$. Expands the derivatives terms using FW as

$$\frac{d^{\alpha}\mu}{dx^{\alpha}} = \sum_{m=0}^{M-1}\sum_{n=1}^{2^{k-1}} d_{m,n}U_{n,m}(x) = (D)^{T}U(x). \tag{6.7}$$

Integrating (6.7) and using initial conditions we obtain

$$\mu(x) = \sum_{m=0}^{M-1}\sum_{n=1}^{2^{k-1}} d_{m,n}(I_{0}^{\alpha}U_{n,m}(x)) + \mu(0) = (D)^{T}P^{\alpha}U(x) + 0.1. \tag{6.8}$$

Substituting (6.7) and (6.8) in (6.6) we have

$$(D)^{T}U(x) + 2.2(D)^{T}P^{\alpha}U(x) + ((D)^{T}P^{\alpha}U(x))^{2} = 2.2. \tag{6.9}$$

After solving the system of Eq. (6.9) using matlab f-solve command we find the unknown coefficient and substitute in (6.8) to find the approximate solutions. In Fig. 7 we have shown the comparison of variation iteration method (VIM)[39] and FWM. The obtained results indicates that FWM are effective for solving linear and non-linear FROM.

7. Conclusion

In this paper, we have developed an effective numerical method based on FW to solve FROM. By employing block-pulse functions, we created FW fractional-order operational matrices of integration. The FROM were reduced to a systems of equations, which are computed by the Newton iteration method. We solved the six test problems both linear and non-linear concerning a minimum level of resolution to strengthen our results. The obtained results are compared with the exact solution and other existing numerical methods such as the DTM,[26] HAM,[20] GTMM,[24,38] and VIM[39] to check the efficiency and accuracy of FWM. The convergence analysis for the proposed method is drawn in terms of the theorems. The absolute error is calculated in Table 1–4 and are compared with the existing literature. Fig. 1–7 presents the approximate solutions graphically for the particular value of the fractional parameter α. Different values of the parameters α are

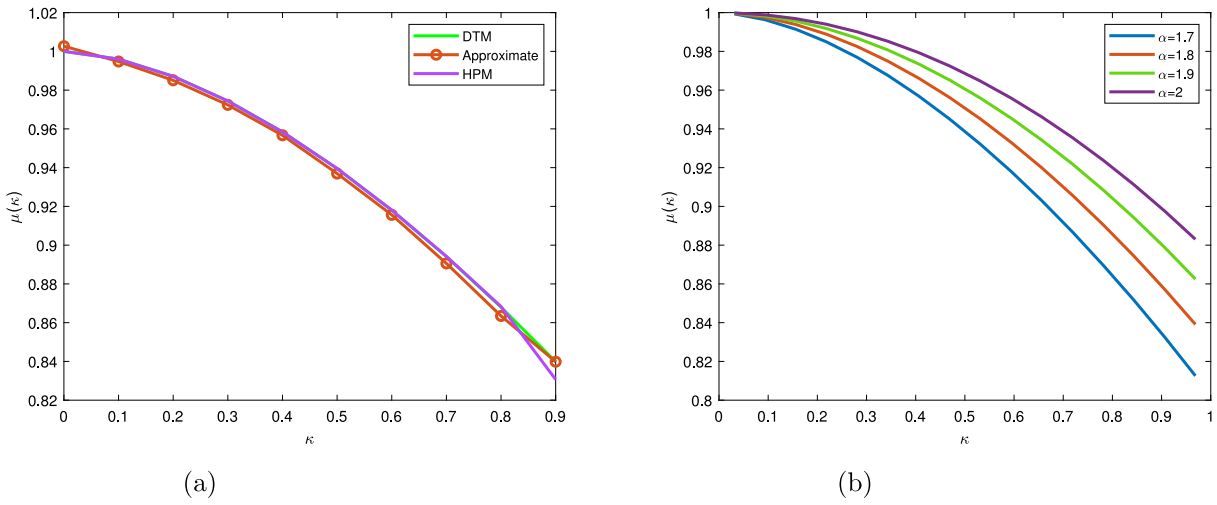

Fig. 5. Comparison of approximate solution and behaviour at different values of α.

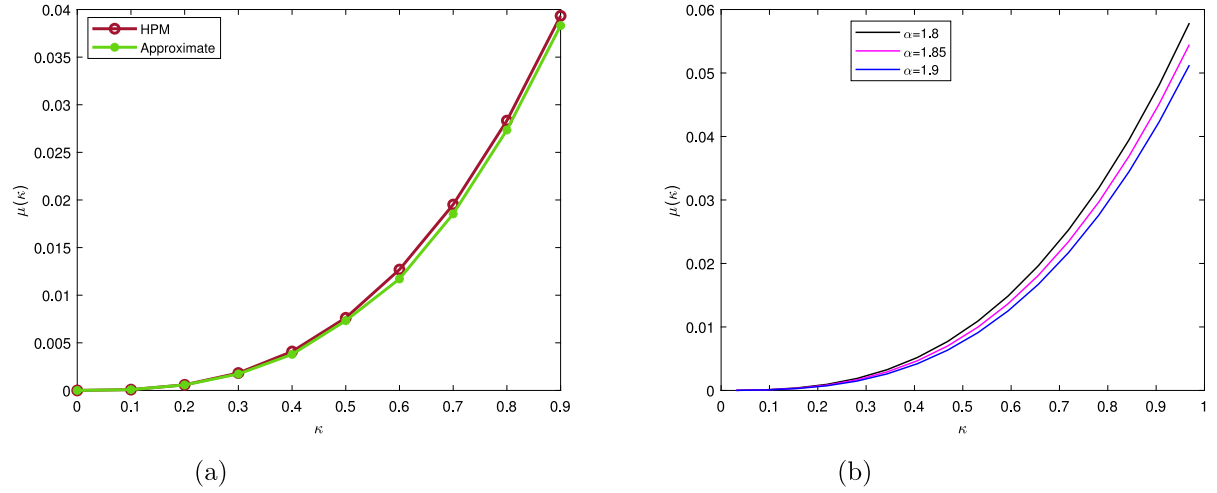

Fig. 6. Comparison of approximate solution and behaviour at different values of α.

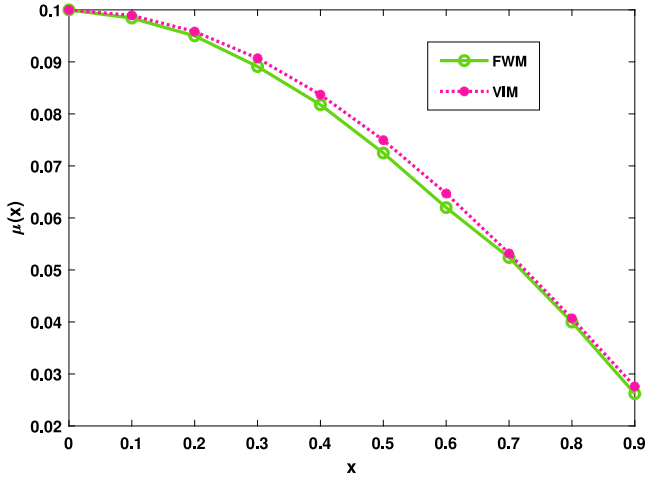

Fig. 7. Comparison of FWM and variation iteration method (VIM) at $\alpha = 1.5$.

used to illustrate how well the FW collocation approach works. The findings of this study indicate that the combination of Caputo fractional derivatives and FWM offers a reliable and robust numerical approach for investigating fractional order dynamics in FROM. This method offers a strong and useful choice for effectively analysing these kinds of FDEs and can be applied to similar problems. In future one can use this method to solve fractional order models, fractional integrodifferential equations and system of ordinary differential equations.

Declaration of competing interest

The authors declare that they have no known competing financial interests or personal relationships that could have appeared to influence the work reported in this paper.

Data availability

No data was used for the research described in the article.

Acknowledgements

We are highly thankful to Central University of Haryana for providing basic facilities to carry out this research. Also this study is supported via funding from Prince Sattam bin Abdulaziz University project number (PSAU/2023/R/1444).

References

1. Kumar S, Kumar R, Osman MS, Samet B. A wavelet based numerical scheme for fractional order SEIR epidemic of measles by using Genocchi polynomials. *Numer Methods Partial Differ Equ*. 2021;37(2):1250–1268.
2. Yadav P, Jahan S, Shah K, Peter OJ, Abdeljawad T. Fractional-order modelling and analysis of diabetes mellitus: Utilizing the Atangana-Baleanu Caputo (ABC) operator. *Alex Eng J*. 2023;81:200–209.
3. Abd-Elhameed WM, Youssri Y. Spectral tau algorithm for certain coupled system of fractional differential equations via generalized Fibonacci polynomial sequence. *Iran J of Sci and Technol Trans Sci*. 2019;43:543–554.
4. Abd-Elhameed WM, Youssri YH. A novel operational matrix of Caputo fractional derivatives of Fibonacci polynomials: Spectral solutions of fractional differential equations. *Entropy*. 2016;18(10):345.
5. Atta AG, Moatimid GM, Youssri YH. Generalized Fibonacci operational Tau algorithm for fractional Bagley–Torvik equation. *Prog Fract Differ Appl*. 2020;6(3):215–224.
6. Youssri YH. Two Fibonacci operational matrix pseudo-spectral schemes for non-linear fractional Klein–Gordon equation. *Int J Mod Phys C*. 2022;33(04):2250049.
7. Khan MA, Ullah S, Kumar S. A robust study on 2019-nCOV outbreaks through non-singular derivative. *Eur Phys J Plus*. 2021;136:1–20.
8. Chen W, Zhang XD, Korosak D. Investigation on fractional and fractal derivative relaxation-oscillation models. *Int J Nonlinear Sci Numer*. 2010;11(1):3–10.
9. Kumar S, Kumar A, Samet B, Gômez-Aguilar JF, Osman MS. A chaos study of tumor and effector cells in fractional tumor-immune model for cancer treatment. *Chaos Solit Fractals*. 2020;141:110321.
10. Kumar S, Chauhan RP, Momani S, Hadid S. Numerical investigations on COVID-19 model through singular and non-singular fractional operators. *Numer Methods Partial Differ Equ*. 2020.
11. Kumar S, Kumar A, Samet B, Dutta H. A study on fractional host-parasitoid population dynamical model to describe insect species. *Numer Methods Partial Differ Equ*. 2021;37(2):1673–1692.
12. Kumar S, Kumar R, Cattani C, Samet B. Chaotic behaviour of fractional predator–prey dynamical system. *Chaos Solit Fractals*. 2020;135:109811.
13. Adolfsson K, Enelund M, Olsson P. On the fractional order model of viscoelasticity. *Mech Time-Depend Mater*. 2005;9:15–34.
14. Enelund M, Olsson P. Damping described by fading memory-analysis and application to fractional derivative models. *Int J Solids Struct*. 1999;36(7):939–970.
15. Bagley RL, Torvik PJ. Fractional calculus-a different approach to the analysis of viscoelastically damped structures. *AIAA J*. 1983;21(5):741–748.
16. Mainardi F. Fractional relaxation-oscillation and fractional diffusion-wave phenomena. *Chaos Solit Fractals*. 1996;7(9):1461–1477.
17. Yang TQ. *Theory of Viscoelasticity*. Wuhan, China: Huazhong Science and Technology University Press; 1990.
18. Tofighi A. The intrinsic damping of the fractional oscillator. *Phys A: Stat Mech Appl*. 2003;329(1–2):29–34.
19. Yadav P, Jahan S, Nisar KS. Solving fractional Bagley–Torvik equation by fractional order FW arising in fluid mechanics. *Ain Shams Eng J*. 2023:102299.
20. Hamarsheh M, Ismail A, Odibat Z. Optimal homotopy asymptotic method (HAM) for solving fractional relaxation-oscillation equation. *J Interpolat Approx Sci Comput*. 2015;2:98–111.
21. Muhammadhaji A, Halik A. Dynamic analysis of a model for Spruce Budworm populations with delay. *J Funct Spaces*. 2021;2021:1–7.
22. Saha T, Pal PJ, Banerjee M. Relaxation oscillation and canard explosion in a slow-fast predator–prey model with Beddington–DeAngelis functional response. *Nonlinear Dynam*. 2021;103:1195–1217.
23. Maleknejad K, Rashidinia J, Eftekhari T. Numerical solutions of distributed order fractional differential equations in the time domain using the Müntz-Legendre wavelets approach. *Numer Methods Partial Differ Equ*. 2021;37(1):707–731.
24. Izadi M. A computational algorithm for simulating fractional order relaxation-oscillation equation. *SeMA J*. 2022;79(4):647–661.
25. Admon MR, Senu N, Ahmadian A, Majid ZA, Salahshour S. A new accurate method for solving fractional relaxation-oscillation with Hilfer derivatives. *J Comput Appl Math*. 2023;42(1):10.
26. Al-rabtah A, Ertürk VS, Momani S. Solutions of a fractional oscillator by using differential transform method (DTM). *Comput Math Appl*. 2010;59(3):1356–1362.
27. Yildirim A, Momani S. Series solutions of a fractional oscillator by means of the homotopy perturbation method. *Int J Comput Math*. 2010;87(5):1072–1082.
28. Lepik Ü, Hein H. Haar wavelets. In: *Haar Wavelets: With Applications*. Cham: Springer International Publishing; 2014:7–20.
29. Rehman M, Saeed U. Gegenbauer wavelets operational matrix method for fractional differential equations. *J Korean Math Soc*. 2015;52(5):1069–1096.
30. Sabermahani S, Ordokhani Y. Fibonacci wavelets and Galerkin method to investigate fractional optimal control problems with bibliometric analysis. *J Vib Control*. 2021;27(15–16):1778–1792.
31. Sabermahani S, Ordokhani Y, Yousefi SA. Fibonacci wavelets and their applications for solving two classes of time-varying delay problems. *Optim Control Appl Methods*. 2020;41(2):395–416.
32. Ahmed S, Shah K, Jahan S, Abdeljawad T. An efficient method for the fractional electric circuits based on Fibonacci wavelet. *Results Phys*. 2023:106753.
33. Chen CF, Hsiao CH. Haar wavelet method for solving lumped and distributed-parameter systems. *IEE Proc Control Theory Appl*. 1997;144(1):87–94.
34. Zada L, Aziz I. Numerical solution of fractional partial differential equations via Haar wavelet. *Numer Methods Partial Differ Equ*. 2022;38(2):222–242.
35. Yadav P, Jahan S, Nisar KS. Fibonacci wavelet collocation method for Fredholm integral equations of second kind. *Qual Theory Dyn Syst*. 2023;22(2):82.
36. Ahmed S, Jahan S, Nisar KS. Hybrid Fibonacci wavelet method to solve fractional-order logistic growth model. *Math Methods Appl Sci*. 2023:1–14.
37. Debnath L. A brief historical introduction to fractional calculus. *Internat J Math Ed Sci Tech*. 2004;35(4):487–501.
38. ülsu M, Öztürk Y, Anapali A. Numerical approach for solving fractional relaxation-oscillation equation. *Appl Math Model*. 2013;37(8):5927–5937.
39. Ahmad J, Mohyud-Din ST. An efficient approach for nonlinear oscillator equations using Jumarie's fractional derivative. *Int J Basic Sci Appl Res*. 2013;2(9):804–809.